



New Tools Provide New Insights in NMR Studies of Protein Dynamics

Anthony Mittermaier, *et al.*

Science **312**, 224 (2006);

DOI: 10.1126/science.1124964

The following resources related to this article are available online at www.sciencemag.org (this information is current as of November 6, 2008):

Updated information and services, including high-resolution figures, can be found in the online version of this article at:

<http://www.sciencemag.org/cgi/content/full/312/5771/224>

A list of selected additional articles on the Science Web sites **related to this article** can be found at:

<http://www.sciencemag.org/cgi/content/full/312/5771/224#related-content>

This article **cites 30 articles**, 6 of which can be accessed for free:

<http://www.sciencemag.org/cgi/content/full/312/5771/224#otherarticles>

This article has been **cited by** 86 article(s) on the ISI Web of Science.

This article has been **cited by** 13 articles hosted by HighWire Press; see:

<http://www.sciencemag.org/cgi/content/full/312/5771/224#otherarticles>

This article appears in the following **subject collections**:

Biochemistry

<http://www.sciencemag.org/cgi/collection/biochem>

Information about obtaining **reprints** of this article or about obtaining **permission to reproduce this article** in whole or in part can be found at:

<http://www.sciencemag.org/about/permissions.dtl>

78. M. Hofmann, C. Eggeling, S. Jakobs, S. W. Hell, *Proc. Natl. Acad. Sci. U.S.A.* **102**, 17565 (2005).
 79. A. Egner, S. W. Hell, *Trends Cell Biol.* **15**, 207 (2005).
 80. M. G. Gustafsson, *Proc. Natl. Acad. Sci. U.S.A.* **102**, 13081 (2005).
 81. W. R. Zipfel, R. M. Williams, W. W. Webb, *Nat. Biotechnol.* **21**, 1369 (2003).
 82. F. Helmchen, W. Denk, *Nat. Methods* **2**, 932 (2005).
 83. P. S. Tsai et al., *Neuron* **39**, 27 (2003).
 84. P. J. Keller, F. Pampaloni, E. H. Stelzer, *Curr. Opin. Cell Biol.* **18**, 117 (2006).
 85. V. Ntziachristos, J. Ripoll, L. V. Wang, R. Weissleder, *Nat. Biotechnol.* **23**, 313 (2005).
 86. P. A. Clemons, *Curr. Opin. Chem. Biol.* **8**, 334 (2004).
 87. We apologize that many original research papers could not be cited because of space limitations. Work by the authors directly related to this review is supported by NIH RR04050, NS27177, GM 72033, and by the Howard Hughes Medical Institute.

10.1126/science.1124618

REVIEW

New Tools Provide New Insights in NMR Studies of Protein Dynamics

Anthony Mittermaier¹ and Lewis E. Kay²

There is growing evidence that structural flexibility plays a central role in the function of protein molecules. Many of the experimental data come from nuclear magnetic resonance (NMR) spectroscopy, a technique that allows internal motions to be probed with exquisite time and spatial resolution. Recent methodological advancements in NMR have extended our ability to characterize protein dynamics and promise to shed new light on the mechanisms by which these molecules function. Here, we present a brief overview of some of the new methods, together with applications that illustrate the level of detail at which protein motions can now be observed.

NMR spectroscopy is an experimental tool developed over half a century ago by physicists who were interested in exploring fundamental properties of matter. They could have hardly imagined the wide utility of their creation. One such example is in the area of structural biology, where since the early 1970s the technique has been used to study the interplay between biomolecular structure, dynamics, and function. An early experiment by Wagner and Wüthrich (1) foreshadowed the importance of NMR in protein science. In this seminal contribution, the authors studied the positions and intensities of peaks in one-dimensional (1D) ¹H NMR spectra of aromatic residues in a small globular protein as a function of temperature and found compelling evidence for rotation of bulky aromatic side chains within the hydrophobic core. This showed that proteins were in fact dynamic over a spectrum of time scales and complemented the beautiful and static pictures of protein structure that were already emerging from x-ray diffraction. We now know that there is an intimate relation between dynamics and molecular function. For example, protein dynamics contribute to the thermodynamic stability of functional states and play an important role in catalysis, where conformational rearrangements can juxtapose key catalytic residues; in ligand binding, which often involves the entry of molecules into areas that would normally be occluded; in molecular recognition processes, which are often

fine-tuned by disorder-to-order transitions; and in allostery, where coupled structural fluctuations can transmit information between distant sites in a protein. NMR spectroscopy is uniquely suited to study many of these dynamic processes, because site-specific information can be obtained for motions that span many time scales, from rapid bond librations (picoseconds) to events that take seconds (2, 3). Here, we review a number of recent advances in solution NMR spectroscopy that have substantially extended our ability to measure protein motions and that promise to improve our understanding of protein dynamics and their relation to biological activity.

Investigating Micro- to Millisecond Time Scale Dynamics

Many biochemical events occur on the microsecond to millisecond time scale, and it is of considerable interest to characterize the conformational transitions that are involved in such processes. However, intermediates are often formed only transiently and are populated at levels that are not amenable to traditional structural approaches. Figure 1 illustrates the situation schematically for the case of a protein that can exist in two distinct conformational states, $A \xrightleftharpoons[k_{BA}]{k_{AB}} B$, with one state substantially more populated than the other. Because the frequency

of the magnetic energy absorbed by each nucleus depends on its chemical environment, a given probe will likely have distinct chemical shifts in each conformation, separated by $\Delta\nu$ (Fig. 1A). If the exchange rate, $k_{ex} = k_{AB} + k_{BA}$, between conformers is very much less than $2\pi\Delta\nu$, then separate peaks may be observed for a single site in each of the conformations, so long as the population of the minor species is on the order of a few percent. However, for systems where k_{ex} is not much smaller than $2\pi\Delta\nu$, peaks derived from the weakly populated conformer (excited state) are most often not observed, because the transient nature of this state leads to substantial peak broadening. As a result, a spectrum is obtained (Fig. 1B) where for each probe a peak is observed only from the more populated state, slightly shifted from its position in the absence of a slow exchange limit. How, then, does one obtain information about the excited state when it is essentially invisible in NMR spectra?

One way is to use an experimental approach, based on an idea from Erwin Hahn in the 1950s, called a spin echo. The basic phenomenon can be explained as follows. Imagine that a group of runners, composed of both slow and fast individ-

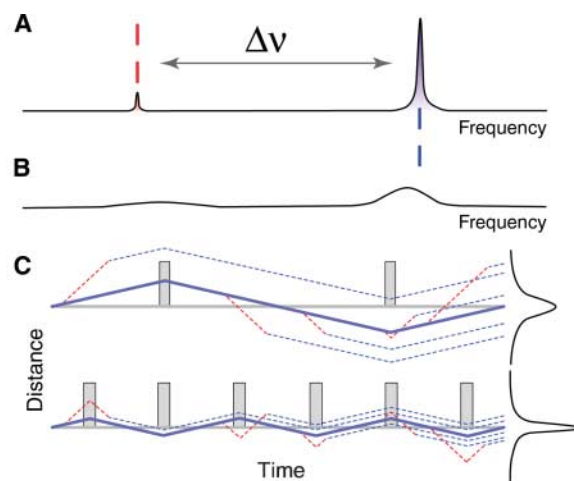


Fig. 1. Spectra from a single protein site undergoing (A) slow conformational exchange, $k_{ex} \ll 2\pi\Delta\nu$, and (B) intermediate conformational exchange, $k_{ex} \approx 2\pi\Delta\nu$. (C) Schematic representation of signal dephasing during CPMG pulse trains based on the analogy to the runners described in the text, where the y axis plots the distance of the runners from the starting position. A blue or red line indicates a spin in the major or minor state, respectively. Dashed lines correspond to spins experiencing at least one conformational transition, whereas the solid lines correspond to no transitions.

¹Department of Chemistry, McGill University, Montreal, Quebec H3A 2K6, Canada. E-mail: anthony.mittermaier@mcgill.ca ²Department of Medical Genetics, Department of Biochemistry, and Department of Chemistry, University of Toronto, Toronto, Ontario M5S 1A8, Canada. E-mail: kay@pound.med.utoronto.ca

uals, start a race at the same time. If at the halfway point of the race all runners are made to stop, turn around, and run back to the starting position, it is clear that both slow and fast individuals will cross the starting line at the same time, giving rise to a spontaneous ordering referred to as an echo. Now suppose that the runners can interconvert stochastically during the course of the race, in the sense that a slow runner can become fast and vice versa (corresponding to molecules interconverting between a pair of states). Although the positions of the runners at the end will depend on the details of the exchange process, in general they will not all finish the race simultaneously, and a plot of the distribution of runners crossing the starting line versus time gives rise to a peak that is broader than that observed in the absence of exchange. The breadth of the peak provides information about the relative numbers of fast and slow runners (thermodynamics), their rate of interconversion (kinetics), and the difference in running speeds between the two groups (analogous to chemical shift differences between exchanging conformations, which relate to structure). The basic NMR experiment [so-called Carr-Purcell-Meiboom-Gill (CPMG) relaxation dispersion (3)] builds on this concept by applying a variable number of refocusing pulses during a fixed time interval, where each pulse corresponds to runners stopping and turning around in the analogy above. If the rate of application of pulses is such that the runners are allowed to get out of phase with each other, then the exchange process leads to broad lines as described above (Fig. 1C, top). In contrast, when the pulses are applied at a fast rate the effects of the interconversion are reduced and narrower peaks are obtained (Fig. 1C, bottom). The dependence of line width on pulsing rate (the relaxation dispersion profile) is subsequently fit to extract the exchange parameters (3).

As mentioned above, the basic CPMG scheme dates back to the formative days of NMR spectroscopy. However, the routine application of the method to proteins had to await a number of advances. One such advance was the development of multidimensional spectroscopy, where the great majority of sites in the protein can, in principle, be visualized in the form of cross peaks in ^1H - ^{15}N or ^1H - ^{13}C

correlation spectra. Such spectra provide the site-specific information that distinguishes modern NMR from so many other physical techniques. The second breakthrough was due to Loria and Palmer, who developed a clever scheme for allowing slow dynamical processes to be charac-

ter, in the context of a ^1H - ^{15}N spin pair, there are additional transitions that can be explored to gain further insight into the dynamics. A comparison of experimental dispersion profiles for the same amide site but derived from experiments that monitor different transitions (Fig. 2A) emphasizes that the same exchange process can lead to very different dispersion shapes (7, 8). Here $R_{2,\text{eff}}$ (peak line width) is plotted along y , versus ν_{CPMG} (proportional to the number of refocusing pulses applied) along x .

CPMG relaxation dispersion experiments in which exchange effects are quenched through the application of pulses are often the method of choice for the study of millisecond dynamics in proteins (3). A similar quenching effect can be achieved by applying a continuous radio-frequency field that is allowed to vary both in magnitude and in frequency (3), and this approach is used to study faster processes (k_{ex} up to $\approx 100,000 \text{ s}^{-1}$).

In order to illustrate the utility of the dispersion methodology, we focus on a single application in the area of protein folding that makes use of the CPMG method (9); additional studies can be found in the literature, with the work of Kern and colleagues relating protein dynamics to enzyme catalysis being particularly noteworthy (10–14). The present example concerns several Gly⁴⁸ mutants of the Fyn SH3 domain that had been shown with use of stopped-flow fluorescence denaturation and renaturation measurements to fold with a two-state

mechanism, $F \xrightleftharpoons[k_{UF}]{k_{FU}} U$. The exchange parameters obtained by using fluorimetry are well within the ranges of k_{ex} values (several hundred to a few thousand s^{-1}) and excited state populations ($p_U > \sim 0.5\%$) that are necessary for the measurement of NMR relaxation dispersions. Yet ^{15}N CPMG studies of a pair of these mutants, Gly⁴⁸→Met⁴⁸ (G48M) and Gly⁴⁸→Val⁴⁸ (G48V), performed in the absence of denaturant, are

inconsistent with a two-state folding mechanism (9). Folding and unfolding rates obtained on a per-residue basis from fits of the dispersion profiles to a two-state folding model do not give the same values at each site, with differences as large as a factor of 10 in some cases; for cooperative folding, k_{UF} and k_{FU} values

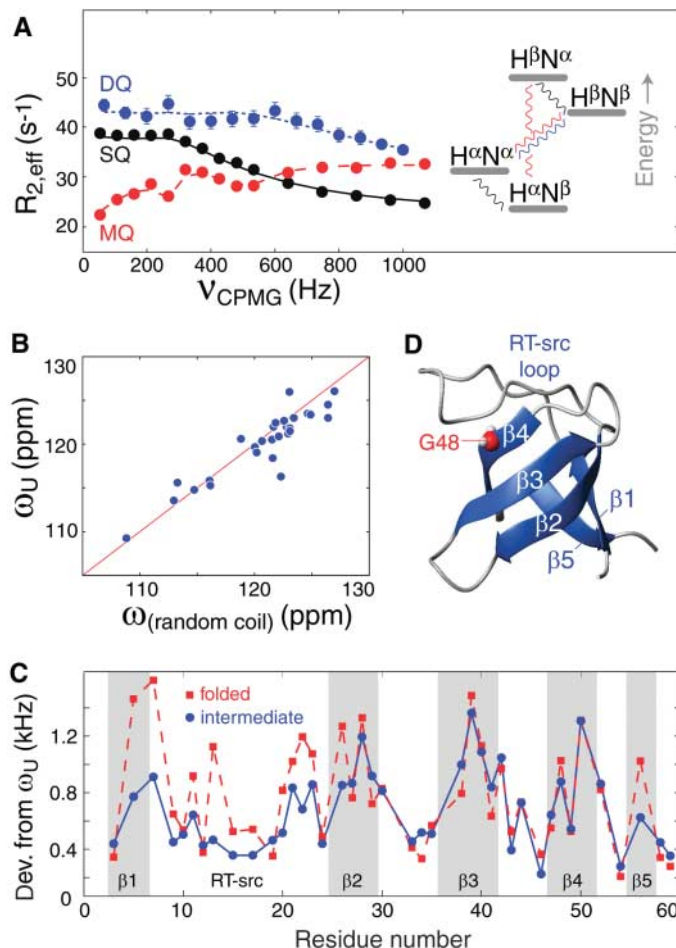


Fig. 2. (A) Experimental relaxation dispersion profiles for amide ^1H - ^{15}N single-quantum (SQ), double-quantum (DQ), and multiple-quantum (MQ) coherences of Glu¹¹ in the G48M mutant of the Fyn SH3 domain (8). Fits to a global three-site model of exchange are indicated by lines. (Inset) An energy level diagram for a ^1H - ^{15}N spin pair with SQ, DQ, MQ coherences indicated by black, blue, and sum of red lines, respectively. (B) The ^{15}N chemical shifts of the G48M U state calculated from relaxation dispersion data plotted as a function of corresponding random coil chemical shifts. (C) Deviations from unfolded (U) state backbone chemical shifts, $\{[\Delta\omega(^{15}\text{N})]^2 + [\Delta\omega(^1\text{H})]^2\}^{0.5}$, calculated in absolute frequency units (800-MHz spectrometer) for intermediate (I, solid blue) and folded (F, dashed red) states, plotted as a function of residue number (8). (D) Structure of the wild-type Fyn SH3 domain (1SHF) with the location of Gly⁴⁸ indicated in red.

terized without interference from interactions between the nucleus of interest and directly bonded NMR-active nuclei (3). CPMG relaxation dispersion experiments most often make use of backbone amide ^1H or ^{15}N spin probes (4–6), focusing on proton or nitrogen magnetization (single-quantum transitions), respectively. How-

are expected to be uniform among all sites in the protein. However, the data for all of the sites in both mutants can be well fit globally to a three-site model of conformational exchange, $F \xrightleftharpoons[k_{IF}]{k_{FI}} I \xrightleftharpoons[k_{UI}]{k_{IU}} U$ (Fig. 2A). The temperature dependence of the four rates allows values of free energy, enthalpy, and entropy differences to be extracted between pairs of states as well as activation barriers, assuming that the temperature dependence of the rates obeys transition state theory (9).

Further information is obtained in the form of chemical shift differences between the *F*, *I*, and *U* states. In fits of the dispersion data, no assumption is made a priori as to the positions of the *I* and *U* states along the reaction scheme; the chemical shifts obtained for an end point state are found to correspond to those of an unfolded protein (i.e., the *U* state) (Fig. 2B). It is well known that chemical shifts are sensitive indicators of molecular structure, and a long-standing goal is to exploit shifts of NMR “invisible” excited states so that structural information can be obtained. The deviations in chemical shifts of the *I* and *F* states from those of *U*, obtained for the G48M Fyn SH3 domain (Fig. 2C), show that the central β sheet is largely formed in the *I* state (β_2 , β_3 , and β_4) but that there is considerably less structure at the termini of the domain. For reference, the *F* state structure of the domain is also illustrated (Fig. 2D).

Measuring Dynamics on the Pico- to Nanosecond Time Scale

Consider a protein that is tumbling in solution such that every orientation is equally probable. For the moment, let us focus on a single bond vector in the molecule that connects a pair of NMR active spins, such as a ^1H - ^{15}N spin pair. When internal motions and molecular tumbling cause reorientation of the ^1H - ^{15}N bond vector with respect to the external magnetic field, the local magnetic field at the site of the ^{15}N spin that derives from the directly attached ^1H magnetic dipole fluctuates (Fig. 3A). It can be shown that, although the local dipolar interaction between ^1H and ^{15}N spins averages to zero because of the molecular tumbling, the time-dependent variations in the field lead a spin system that

has been perturbed by radio-frequency pulses to return, or relax, to thermal equilibrium. Because the fluctuations of the local magnetic fields are sensitive to internal motions, measurement of NMR relaxation rates provides a direct avenue to extracting dynamics parameters.

A pair of basic nitrogen spin relaxation experiments are used to probe backbone dynamics

equilibrium value (T_2). The ^1H spin has a magnetogyric ratio (γ) that is 10 times larger than that of ^{15}N , and the inherent sensitivity of the NMR experiment scales as γ^2 ; therefore experimental sensitivity is optimized by shuffling magnetization from an amide ^1H to its directly coupled ^{15}N and then back again to ^1H for detection as a 2D data set. Here, one peak is obtained for each (^1H - ^{15}N) pair in the protein, with an intensity proportional to $\exp(-\tau/T_i)$ where T_i is the T_1 or T_2 value of the particular ^{15}N nucleus and τ is a variable relaxation delay; relaxation times are measured by recording a series of spectra and fitting the peak intensities as a function of τ . The values of T_i so obtained are usually interpreted in terms of generalized order parameters that describe the amplitude of bond vector motions and time constants that indicate the time scale of the internal motions (15), but specific models can be used as well (16). In addition, many experiments that provide complementary information to the ^{15}N studies described above have been developed, such as those that measure correlated motions of successive residues in proteins (17, 18) or the dynamics of backbone carbonyl-C α bonds (19).

Side chain motions in proteins are also amenable to study with the use of spin relaxation techniques (20, 21). In particular, the use of the ^2H nucleus as a probe of side chain methyl group dynamics has seen substantial advances in recent years. It has long been known that the deuterium spin is an excellent probe of molecular motion, but applications in the solution state were limited, primarily because the poor resolution of ^2H spectra make site-specific studies extremely difficult. This is illustrated by protein spectra in Fig. 3C, where the broad, featureless 1D ^2H spectrum may be compared with the high resolution ^1H spectrum. The deuterium can be exploited as a probe of molecular dynamics, however, by preparing uniformly ^{13}C labeled, fractionally deuterated protein and using the scheme illustrated in Fig. 3D that can be “tuned” to select, in this case, for $^{13}\text{CH}_2\text{D}$ methyl groups. A series of high resolution ^{13}C - ^1H maps are produced, with ^2H relaxation rates encoded by the intensities of the cross peaks.

One of the most exciting applications of the methodology described above is in the use of

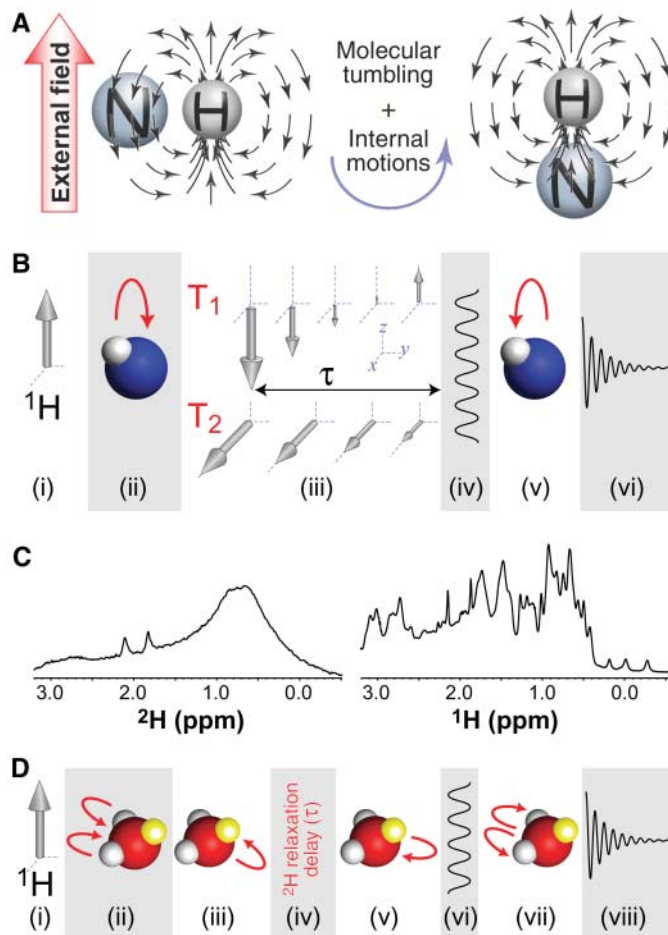


Fig. 3. (A) Illustration of the orientation-dependent magnetic field experienced by an amide ^{15}N nucleus due to the directly bonded proton. A pair of orientations have been chosen arbitrarily for illustration. (B) Schematic representation of an amide ^{15}N relaxation experiment (2): (i) equilibrium ^1H magnetization, (ii) ^1H to ^{15}N transfer, (iii) relaxation delay, (iv) indirect ^{15}N chemical shift detection, (v) ^{15}N to ^1H transfer, and (vi) direct ^1H chemical shift detection. (C) 1D ^2H and ^1H spectra of perdeuterated and protonated spectrin SH3 domains, respectively. (D) Schematic representation of a methyl ^2H relaxation experiment (21): (i) equilibrium ^1H magnetization, (ii) ^1H to ^{13}C transfer, (iii) ^{13}C to ^2H transfer, (iv) relaxation delay, (v) ^2H to ^{13}C transfer, (vi) indirect ^{13}C chemical shift detection, (vii) ^{13}C to ^1H transfer, and (viii) direct ^1H chemical shift detection.

in proteins (2) (Fig. 3B). Although a large arsenal of different methods have now been developed, most are fundamentally similar to this example. The ^{15}N relaxation experiments monitor either the recovery of ^{15}N Z-magnetization to its equilibrium position (T_1) or the decay of magnetization orthogonal to the Z axis to its zero

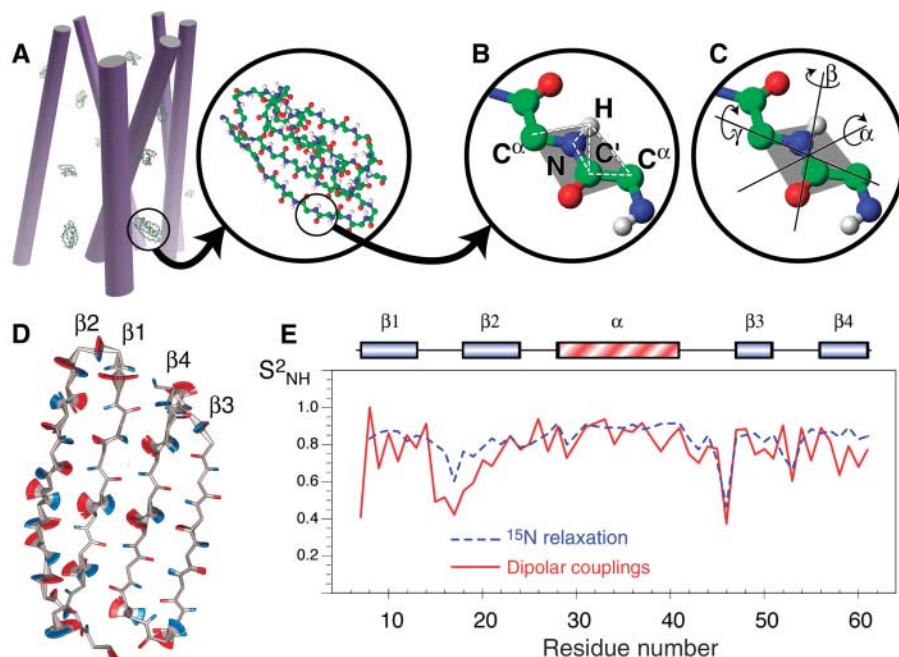


Fig. 4. (A) Representation of protein G B1 domain molecules dissolved in an anisotropic medium, with cylinders corresponding to filamentous phage particles aligned with respect to the static magnetic field. (B) Peptide plane with spin pairs, for which residual dipolar coupling data was obtained, identified by dashed white lines. (C) The three axes of rotation for a GAF model of rigid-body peptide plane dynamics. (D) Visualization of γ rotations for peptide planes in the β sheet. (E) Comparison of ^{15}N relaxation-derived “fast motion” order parameters and residual dipolar coupling-derived order parameters. [Figure adapted from Bouvignies *et al.* (28); copyright (2005), National Academy of Sciences, United States]

order parameters as restraints in molecular dynamics calculations to produce an ensemble of structures that satisfies both structural and dynamical NMR data. In one such study involving ubiquitin, it was found that many side chains, even those in the core of the protein, occupy multiple rotameric states and can be considered to have liquidlike characteristics (22).

Probing Dynamics Spanning a Broad Time Scale Range by Using Residual Dipolar Couplings

Let us return to the example of the ^1H - ^{15}N spin pair in Fig. 3A, but now suppose that the protein is not dissolved in isotropic solution but rather in a media that leads to fractional alignment (typically about 0.1%) (23) (Fig. 4A). In this case, the dipolar interaction considered above does not average to zero. Instead, for a fixed orientation of the ^1H - ^{15}N spin vector, the effective magnetic field at the ^{15}N spin is either increased or decreased depending on the ^1H spin state, leading to dipolar splittings (^{15}N peak doublets) in spectra. These splittings are a rich source of structural information, because they report on the orientation of bond vectors with respect to an external coordinate frame (the magnetic field) (23). However, there is also potential for studies of biomolecular dynamics because motions that modulate local fields over a broad

time regime (picosecond to millisecond) can affect dipolar splittings (24–27). Here, we focus on one such study by Blackledge and co-workers that highlights beautifully the power of the dipolar coupling approach (28).

In this study, the authors used an extensive set of dipolar couplings recorded on the immunoglobulin-binding B1 domain of streptococcal protein G (protein G). Data from experiments performed in a number of different alignment media were pooled to obtain as many as 27 measurements per residue, with six different types of dipolar couplings measured per peptide plane (Fig. 4B). The dipolar coupling data were interpreted by using the x-ray structure of the protein along with a 3D Gaussian axial fluctuation model (GAF) of the motion (Fig. 4C) (16). A remarkable distribution of motion about the γ axis was found for residues throughout the β sheet of the protein (Fig. 4D), with hydrogen-bonded residues on adjacent strands experiencing similar levels of dynamics. In order to address whether the motions of interacting peptide planes are correlated, the authors recorded three-bond ^{15}N - ^{13}C scalar couplings (^{15}N - ^1H - ^1O - ^{13}C), which depend on lengths and angles of $\text{H}\cdots\text{O}$ hydrogen bonds. Experimental couplings were compared with values calculated by using the GAF fluctuation amplitudes from the dipolar coupling measurements, assuming either correlated, anticor-

related, or uncorrelated motion. Significantly better agreement between computed and experimental couplings was obtained for the correlated motional model compared with the other two models. Although dipolar coupling data per se do not report on the time scale of motion, information can be obtained by comparing the per-residue generalized order parameters from the 3D GAF model of dynamics with order parameters extracted from backbone ^{15}N spin relaxation data (see above) that report on pico- to nanosecond time scale motions (Fig. 4E). For the sites involved in the correlated dynamics described above, dipolar coupling-derived generalized order parameters are lower than those obtained from ^{15}N relaxation experiments, implying that the correlated dynamics involve motional time scales that are slower than the pico- to nanosecond range.

Lastly, we note that the residues with the highest level of dynamics are those that interact with the protein G binding partner and that the direction of the motion (about the γ axis) coincides with the conformational adjustment needed for molecular recognition and for the formation of a hydrogen bonded complex.

Concluding Remarks

Over the past several years, new NMR experiments have been developed to provide site-specific information about protein motions spanning a range of time scales. Some of the most exciting new applications involve large molecular complexes, where motion is likely to be critical for function. NMR methods exploiting the TROSY (transverse relaxation optimized spectroscopy) principle (29) have emerged for both backbone positions and side chain methyl groups, allowing site-specific studies of dynamics to be performed on large protein complexes such as the GroEL-GroES chaperone (30) and the ClpP protease (31). It is clear from these studies, and from the applications to the smaller proteins described above, that the insights obtained from NMR dynamics studies will have important implications for our understanding of biological function.

References

1. K. Wüthrich, G. Wagner, *Trends Biochem. Sci.* **3**, 227 (1978).
2. L. E. Kay, D. A. Torchia, A. Bax, *Biochemistry* **28**, 8972 (1989).
3. A. G. Palmer, C. D. Kroenke, J. P. Loria, *Methods Enzymol.* **339**, 204 (2001).
4. J. P. Loria, M. Rance, A. G. Palmer, *J. Am. Chem. Soc.* **121**, 2331 (1999).
5. R. Ishima, D. Torchia, *J. Biomol. NMR* **25**, 243 (2003).
6. M. Tollinger, N. R. Skrynnikov, F. A. A. Mulder, J. D. Forman-Kay, L. E. Kay, *J. Am. Chem. Soc.* **123**, 11341 (2001).
7. D. M. Korzhnev, P. Neudecker, A. Mittermaier, V. Y. Orekhov, L. E. Kay, *J. Am. Chem. Soc.* **127**, 15602 (2005).
8. A. Mittermaier, D. M. Korzhnev, L. E. Kay, *Biochemistry* **44**, 15430 (2005).
9. D. M. Korzhnev *et al.*, *Nature* **430**, 586 (2004).

10. R. Ishima, J. M. Louis, D. A. Torchia, *J. Mol. Biol.* **305**, 515 (2001).
11. M. J. Grey, C. Y. Wang, A. G. Palmer, *J. Am. Chem. Soc.* **125**, 14324 (2003).
12. F. A. A. Mulder, A. Mittermaier, B. Hon, F. W. Dahlquist, L. E. Kay, *Nat. Struct. Biol.* **8**, 932 (2001).
13. M. Wolf-Watz *et al.*, *Nat. Struct. Mol. Biol.* **11**, 945 (2004).
14. E. Z. Eisenmesser *et al.*, *Nature* **438**, 117 (2005).
15. G. Lipari, A. Szabo, *J. Am. Chem. Soc.* **104**, 4546 (1982).
16. T. Bremi, R. Brüschweiler, *J. Am. Chem. Soc.* **119**, 6672 (1997).
17. P. Pelupessy, S. Ravindranathan, G. Bodenhausen, *J. Biomol. NMR* **25**, 265 (2003).
18. P. Lundstrom, F. A. Mulder, M. Akke, *Proc. Natl. Acad. Sci. U.S.A.* **102**, 16984 (2005).
19. T. Wang, K. K. Frederick, T. I. Igumenova, A. J. Wand, E. R. Zuiderweg, *J. Am. Chem. Soc.* **127**, 828 (2005).
20. D. M. LeMaster, D. M. Kushlan, *J. Am. Chem. Soc.* **118**, 9255 (1996).
21. D. R. Muhandiram, T. Yamazaki, B. D. Sykes, L. E. Kay, *J. Am. Chem. Soc.* **117**, 11536 (1995).
22. K. Lindorff-Larsen, R. B. Best, M. A. Depristo, C. M. Dobson, M. Vendruscolo, *Nature* **433**, 128 (2005).
23. N. Tjandra, A. Bax, *Science* **278**, 1111 (1997).
24. J. R. Tolman, J. M. Flanagan, M. A. Kennedy, J. H. Prestegard, *Nat. Struct. Biol.* **4**, 292 (1997).
25. G. M. Clore, C. D. Schwieters, *Biochemistry* **43**, 10678 (2004).
26. J. Meiler, J. J. Prompers, W. Peti, C. Griesinger, R. Brüschweiler, *J. Am. Chem. Soc.* **123**, 6098 (2001).
27. J. J. Chou, D. A. Case, A. Bax, *J. Am. Chem. Soc.* **125**, 8959 (2003).
28. G. Bouvignies *et al.*, *Proc. Natl. Acad. Sci. U.S.A.* **102**, 13885 (2005).
29. K. Pervushin, R. Riek, G. Wider, K. Wüthrich, *Proc. Natl. Acad. Sci. U.S.A.* **94**, 12366 (1997).
30. R. Horst *et al.*, *Proc. Natl. Acad. Sci. U.S.A.* **102**, 12748 (2005).
31. R. Sprangers, A. Gribun, P. M. Hwang, W. A. Houry, L. E. Kay, *Proc. Natl. Acad. Sci. U.S.A.* **102**, 16678 (2005).

10.1126/science.1124964

PERSPECTIVE

Living Cells as Test Tubes

X. Sunney Xie,* Ji Yu, Wei Yuan Yang

The combination of specific probes and advanced optical microscopy now allows quantitative probing of biochemical reactions in living cells. On selected systems, one can detect and track a particular protein with single-molecule sensitivity, nanometer spatial precision, and millisecond time resolution. Metabolites, usually difficult to detect, can be imaged and monitored in living cells with coherent anti-Stokes Raman scattering microscopy. Here, we describe the application of these techniques in studying gene expression, active transport, and lipid metabolism.

Much of our quantitative understanding of molecular reactions in cells has come from traditional biochemistry—experiments done in test tubes with purified biomolecules. Although this approach is extremely productive, we understand that the milieu of the cell is fundamentally different from an *in vitro* solution in several ways: (i) DNA, many mRNA molecules, and some enzymes exist in low copy numbers and participate in stochastic reaction events in the cell that are hidden in test tubes with large numbers of molecules. (ii) Reactions are often at nonequilibrium steady state in the cell, with a constant supply of free energy and reactants. (iii) Many reactions are coupled in the cell, resulting in networks of complex interactions. Consequently, a biochemical reaction in a single cell could have different thermodynamic and kinetic properties from the same biochemical reaction in a test tube. The challenge now is to observe the biochemical reactions in living cells, and techniques are in place to do this in selected systems. Central to these techniques is optical imaging, which offers millisecond time resolution and nanometer spatial precision, single-molecule sensitivity, and most importantly, biochemical specificity. Here, we highlight advances that allow investigation of gene expression, active transport, and metabolism in living cells.

In an individual cell, gene expression is a single-molecule problem. On genomic DNA, a particular gene only exists in one (or a few) copy, switching on and off stochastically to regulate biological functions [for a review, see (1)]. Gene expression has been studied by biochemical assays, such as Northern and Western blotting, polymerase chain reaction, and more recently, DNA arrays and mass spectrometry. However, these techniques are not sensitive enough to allow single-cell analysis of genes that are expressed at low levels. Furthermore, these ensemble-averaged methods often mask stochastic gene expression events. Single-molecule experiments *in vitro* have provided valuable insight into the mechanisms of gene expression machines (2–4). The next frontier will carry out single-molecule studies in individual living cells.

Imaging of gene expression at a single-molecule level in living cells has been made possible by two developments. At the transcriptional level, single mRNA molecules were detected and tracked in a living cell using multiple copies of a fluorescent mRNA binding protein (5, 6). At the translational level, we have tracked expression of single-protein molecules using a fast-maturing and membrane-targeting yellow fluorescent protein (YFP) (Venus) as a reporter (7).

Immobilizing the fluorescent protein reporter on the cell membrane (7, 8) overcame the difficulty in detecting single-protein molecules inside the cytoplasm; the fluorescence distributes throughout the cell because of fast protein diffusion during the image acquisition time and

drops below the strong cellular autofluorescence. We monitored repressed expression from the *lac* promoter in *Escherichia coli* (Fig. 1A) and showed that protein expression occurs in small bursts (Fig. 1B), each originating from multiple ribosomes on an mRNA molecule. The protein copy numbers within a burst adhered to a geometric distribution (7), which was verified with the use of a different reporter (9). These assays provided quantitative details about the stochastic fluctuations in gene expression.

Is there a way to detect a single cytoplasmic protein molecule? The answer is yes, by extending the idea of detection by immobilization. We borrowed a method from strobe photography, which makes it possible to take a sharp picture of a bullet going through an apple (Fig. 1C). The sharpness is achieved because the light flash is so short that the bullet does not move far during the flash. Likewise, we applied an intense laser exposure for a very short duration (~300 μs), during which a protein reporter does not diffuse beyond the diffraction-limited spot. Figure 1D shows detection of single red fluorescent proteins [tdTomato (10)] in *E. coli* cytoplasm with a high signal-to-background ratio. The method could be used, for example, to determine the cellular concentration of a weakly expressed protein without calibration. To further develop this method, we need reporters with high photostability and better-controlled photochemistry.

The next step is to probe the expression of multiple genes simultaneously with the use of different colors of reporters (10) in order to study their interactions. In addition to transcription and translation, similar live-cell single-molecule assays offer the prospect of studying cellular processes, such as cell signaling (11), protein folding, DNA replication, and RNA trafficking (5, 12).

No less important than gene expression is energy transduction in living cells. Motor proteins convert chemical energy in the form of adenosine 5'-triphosphate (ATP) into mechanical work. Kinesin and dynein motors transport organelles along microtubules in opposite directions. Much has been learned about these motors at the single-

Department of Chemistry and Chemical Biology, Harvard University, Cambridge, MA 02138, USA.

*To whom correspondence should be addressed. E-mail: xie@chemistry.harvard.edu